

A red fluorescent protein laser based on microbubble cavity with high stability and ultra-low threshold

JIYANG MA,^{1,2†} SHUOYING ZHAO,^{1,2†} XUBIAO PENG,^{1,2} GAOSHANG LI,^{1,2}
YUANJIN WANG,^{1,2} ZHANGQI YIN^{1,2}, BO ZHANG^{1,2,3} AND QING ZHAO^{1,2,4}

¹Center for Quantum Technology Research and Key Laboratory of Advanced Optoelectronic Quantum Architecture and Measurements (MOE), School of Physics, Beijing Institute of Technology, Beijing 100081, China

²Beijing Academy of Quantum Information Sciences, Beijing 100193, China

³bozhang_quantum@bit.edu.cn

⁴qzhaoyuping@bit.edu.cn

Abstract: Biological lasers show considerable potential in the biomedical field. Fluorescent protein (FP) is a type of biomaterial with good luminescence efficiency that can be used as the luminescent gain medium in biological lasers. Red FPs (RFPs) show higher cell/tissue permeability, lower cell phototoxicity, and relatively less background fluorescence than FPs based on other colors. RFPs can be used in vivo for deep tissue imaging. mCherry is the most extensively used high-quality RFP because of its short maturation time and stable luminescence properties. In this study, we employ mCherry FPs with a whispering gallery mode microbubble cavity to fabricate a protein laser. The laser resonator achieves a maximum quality factor (Q factor) of 10^8 , which is the highest Q factor among the currently available FP lasers. Moreover, this laser exhibits the lowest threshold of 169 fJ, which can effectively ensure that the pump light does not damage the luminescent material. The prepared laser shows excellent stability in a wide pH range with good photobleaching resistance and can be stored at 3 °C for more than a month. This laser can be used to perceive and observe life-related activities in deep tissues of organisms.

1. Introduction

Bioluminescent materials [1-3] show high biocompatibility and biodegradability, including chlorophyll, riboflavin, fluorescent protein and so on. Lasers with biomaterials as gain medium are referred to as biological lasers [4]. Different from the spontaneous emission, the laser generates stimulated radiation amplification of fluorescence through the interaction between optical resonator and bioluminescent materials. Compared with fluorescence, lasers offer the advantages of high brightness, narrow linewidth and high signal-to-noise ratio, which is more suitable for biosensing. Especially, the biological laser based on whispering gallery mode microcavity with high quality factor and ultra-small mode volume facilitating the strong interaction between the bio-element and the optical mode can enhance the sensitivity [5,6]. This kind of biological laser has played an important role in cell tracking [7-9], biological detection [10-20], biological imaging [21] and so on.

Fluorescent proteins (FPs) [22], a nontoxic and biocompatible bioluminescent material, was first found in *Aequorea victoria*, which exhibit large absorption cross section and high fluorescence quantum yield. The mutant of *A. Victoria* can cover the whole visible light band. Owing to these advantages, FPs have been instrumental in the biological field in the recent decades. Currently, FPs used to fabricate biological lasers include green [23-29] and yellow [30] FPs as well as green-red FP pairs [31], which are used to study fluorescence resonance energy transfer (FRET). Red fluorescence shows higher cell tissue permeability, lower cell phototoxicity and relatively less background fluorescence. It can be used for deep tissue

imaging in vivo. Therefore, FPs in the red wavelength regime are beneficial for imaging at different scales, from a single molecule to the entire organism. However, at present, red fluorescent protein (RFP) laser is scarcely explored. mCherry—the most commonly used class of RFP is a mutant derivative of DsRed FP [32] with a short maturation time, good photobleaching resistance, and excellent acid-base stability.

Herein, we employ mCherry RFPs along with a silicon oxide microbubble resonator [33] to fabricate an mCherry FP laser, as schematically shown in Figure 1 (a). For the first time, pure mCherry is used as a luminescent gain medium to fabricate an FP laser. Due to the advantages of mCherry, the prepared laser shows high stability, good photobleaching resistance, good pH stability and can be preserved for a long time. Furthermore, the laser achieves an ultrahigh quality factor (Q factor) of 10^8 , which is the highest Q factor among all the currently available FP lasers. The laser threshold is as low as 169 fJ, at this threshold, the luminescent material can be effectively protected against damage from pump light. Because the microcavity achieves a high Q factor, the output laser can be realized using a 1.13 μM mCherry protein solution, which is the lowest concentration of the gain medium in the currently available FP lasers. The findings of this study will contribute to the understanding of luminescent materials for biological laser applications and guide trace biological detection, fluorescence resonance energy transfer (FRET), and other related fields.

2. MCherry, experimental setup and microbubble preparation:

MCherry is mutated from the earliest red fluorescent protein DsRed. Due to its short maturation time, mCherry is the most widely used monomer red protein at present. MCherry has high stability and photobleaching resistance, and is widely used in cell calibration, cell tracking and so on [34-36]. The 3D structure of mCherry protein is shown in Figure 1 (b).

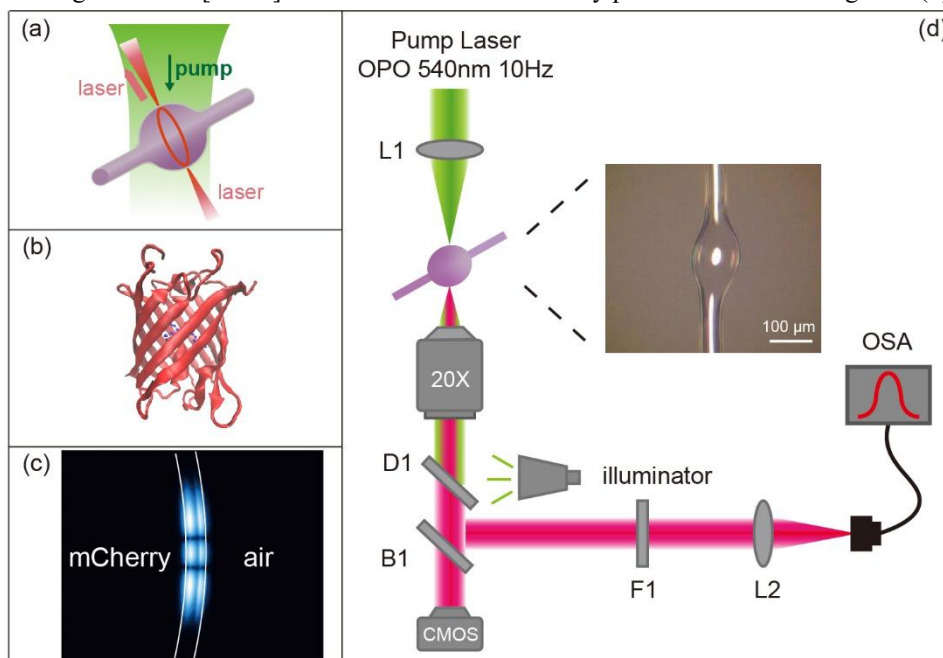


Fig. 1 (a) Schematic diagram of mCherry laser; (b) mCherry protein structure; (PDB ID: 2H5Q[37]) (c) Simulation of optical mode field with mCherry in the microbubble cavity; (d) Schematic diagram of experimental setup: L1 and L2 are convex lenses, D1 is dichroic mirror, which can reflect green light and project red light, B1 is 50% / 50% beam splitter, F1 is long-pass filter, which can pass through red light and block green light

Figure 1 (c) shows the simulation of the optical mode distribution of the microbubble cavity filled with mCherry. It has a diameter of 115 μm and wall thickness of 1.7 μm . Due to the ultrathin wall thickness of the resonator, its mode shows a strong evanescent field, which effectively interacts with mCherry to produce a laser. An experimental setup (Figure 1 (d)) was used to excite mCherry in the microbubble cavity and collect the laser beam generated through the microcavity. The pulse width of the pump light is 7 ns with repetition rate of 10 Hz and wavelength of 540 nm. The pump light adjusts the energy and spot size through the polarizer and the beam expander, then, it passes through the convex lens with a focal length of 20 cm, and finally irradiates the microbubble cavity with a spot size of 1 mm in diameter. The laser is collected through a 20X objective lens. The dichroic lens and long-pass filter were used to filter 540 nm pump light. Finally, an optical fiber was used to collect the red laser beam and transmit it to a spectrum analyzer (Ocean Optics, Model Maya2000 Pro, 1-nm resolution).

The fabrication of the microbubble resonator can be simply described as follow: we select a silica capillary with an inner diameter, outer diameter, and sidewall thickness of 100, 140, and 20 μm , respectively. First, the capillary was immersed in a hot piranha solution (155 ° C) to remove the thin polymer layer on its outer surface. Then, the capillary was immersed in 5% hydrofluoric acid to reduce its sidewall thickness from 20 to 10 μm . The capillary corroded by hydrofluoric acid is drawn from both sides down to an outer diameter of 50 μm under hydrogen flame heating. Next, the inside of the capillary was pressurized and blown into a microbubble cavity under carbon dioxide laser irradiation.

3. Calculation on the excitation frequency of mCherry fluorescence:

Following the photoexcitation model of green FPs (GFPs) [38], we preliminarily calculated the energy level and fluorescence excitation frequency of mCherry under neutral and ionized conditions using the QM/MM method of Orca software [39]. The crystal structure (PDB: 2H5Q) [37] of mCherry was adopted; We take the chromophore part for QM calculation with the base group B3LYP/6-31G, and take the rest regions as the MM calculation area. For the ionized state, the chromophore and residue GLU215 were deprotonated and protonated, respectively, to obtain the initial state. Figure 2 (a) shows the vertical absorption wavelength according to our calculation. The absorption peaks were estimated to be 636 and 545 nm in the neutral and ionized states, respectively. Based on the GFP model, the fluorescence of the protein was produced in the ionized state. Therefore, we used 540-nm pump light to excite the RFP to produce the fluorescence. However, the calculation of the fluorescence spectrum from QM/MM method is difficult and inaccurate due to the dynamics of the excited states, here we directly give the fluorescence spectrum of mCherry from experiment that are deposited in the FP database (FP Base) in Fig. 2 (b). According to the FP Base, the fluorescence quantum yield of mCherry is 0.22 and the maximum emission peak was at ~610 nm [40].

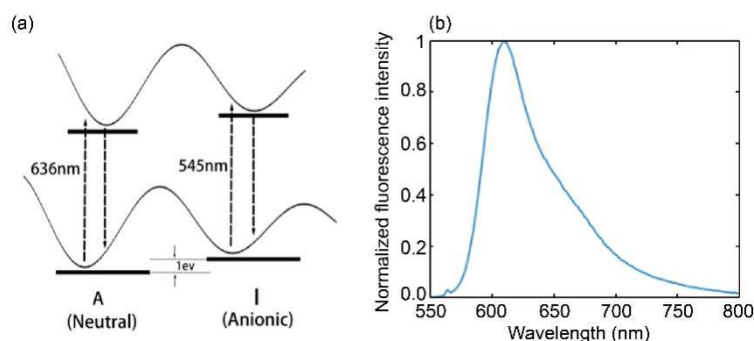


Fig. 2 (a) Calculated vertical absorption peak; (b) mCherry fluorescence emission spectrum

4. Results and discussion:

We prepared a microbubble cavity with a diameter of 115 μm and a wall thickness of 1.7 μm . The inset in figure 1 (d) shows an optical microscopic image of the microbubble cavity. Subsequently, the red fluorescent protein mCherry with concentration 39.7 μM was injected into the microbubble cavity. From the mode field distribution of microbubble cavity theoretically simulated by COMSOL multiphysics software, the optical energy is mainly distributed in the side wall of microbubble cavity. Because the side wall of microbubble cavity is ultrathin, a strong evanescent field is distributed inside the cavity. This part of energy interacts with mCherry gain medium to produce gain effect, as shown in Fig. 1 (c). According to the simulation results, the mode volume of microbubble cavity is only $2.2 \times 10^{-17} \text{ m}^3$, 2.8×10^{-5} of the microbubble cavity volume. The quality factor of the naked microbubble cavity is 1.1×10^8 , which reduced to 10^8 after filled with solution of mCherry, as shown in Fig. 3 (a). Although the Q factor of the microbubble cavity decreased after injection with the mCherry gain medium, it was still sufficiently high. Fig. 3 (b) shows the Normalized laser emission spectra of mCherry protein with concentration of 39.7 μM excited under different pump energy. The wavelength distribution of red laser is in the range of 625 nm to 680 nm, and the laser intensity is the highest at 647.42 nm. Compared with the maximum fluorescence emission peak of mCherry, the different spectral properties between the stimulated and spontaneous emissions induced a slight redshift. Based on the Q factor and diameter of the microcavity, the laser linewidth should be less than 10 fm and the free spectral range should be 0.8 nm. However, the laser emission spectrum presented a wide-band envelope, which is due to the limitation of the resolution of the spectrometer ($\sim 1 \text{ nm}$), the extremely narrow linewidth and discrete laser spectral lines cannot be clearly distinguished. Fig. 3 (c) shows the threshold measurement results of the laser. It can be seen that the threshold of mCherry protein laser is only 0.59 $\mu\text{J}/\text{mm}^2$. Because only the evanescent field inside the microbubble cavity can interact with fluorescent protein, the effective pump energy used in this part is only 169 fJ, which is the lowest threshold among all currently available FP lasers. Threshold is an important parameter to characterize laser. When the threshold is low, the energy required to produce a laser is low. A low threshold and a high gain effect are critical in the application of bio-lasers, which can not only ensure that the bioluminescent materials are resistant to damage caused by the pump light but can also avoid the introduction of other effects in the biological detection processes, such as the thermal effect and nonlinear effect of microcavity's material. The inset in Fig. 3 (b) shows the image of the sample observed and recorded by CMOS camera under the excitation of pump light, confirming the simulation results that the optical mode distributes on the side wall of the microcavity, where the gain medium interacts with the microcavity and produce laser.

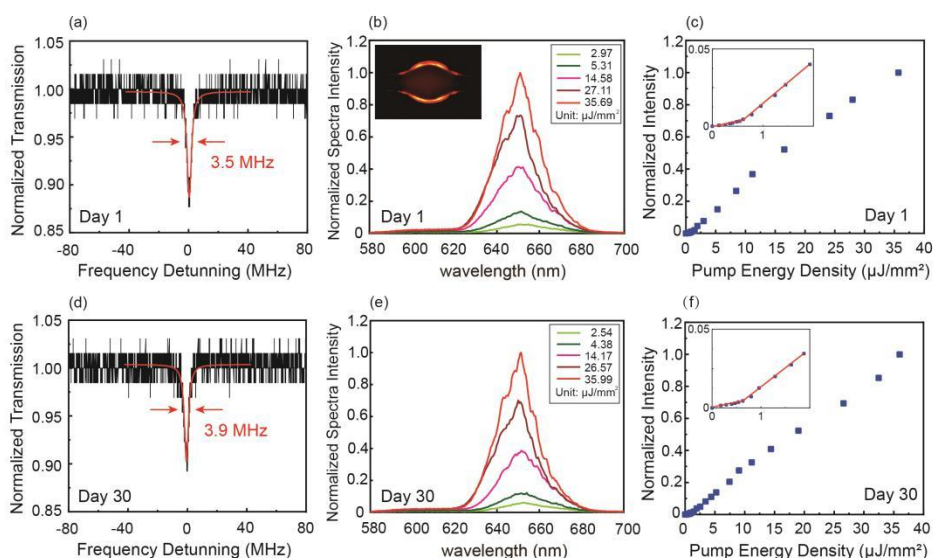


Fig. 3 (a) Initial Lorentz transmission spectrum of mCherry laser, corresponding to Q factor of 10^8 ; (b) Spectrum of mCherry laser under different pump energies; (c) Threshold measurement of mCherry laser; (d) The Lorentz transmission spectrum of mCherry laser after one month, corresponding to the Q factor of 9.8×10^7 ; (e) Spectrum of mCherry laser under different pump energy after one month; (f) Threshold measurement of mCherry laser one month later

The laser exhibited good luminescence stability. We seal both ends of the microbubble cavity with UV glue to ensure that the mCherry is not polluted or evaporated and store it in the sample box to prevent microbubble from contamination. When not used, the sample is stored in a refrigerator at 3 °C. After one month, the luminescence properties of the mCherry protein laser changed slightly while still maintaining the low threshold characteristics. Fig. 3 (d) and (e) respectively shows the Lorentz transmission spectrum of the microcavity and the normalized emission spectrum of the laser under different pump energy after one month. Compared with the data shown in Fig. 3 (a) and (b), no obvious change was observed in the Q factor and spectrum of the microcavity laser. Fig. 3 (f) shows the laser threshold measurement after one month, and the laser threshold is $0.65 \mu\text{J}/\text{mm}^2$. In fact, the preservation time can last even longer, which is not limited to one month's test. The long-term reusability of our mCherry laser is of great significance in practical applications.

Next, we tested the pH stability of the mCherry laser. We changed the pH value of the mCherry FP solution at a consistent concentration. Experiments showed that mCherry protein laser had high pH stability. Fig. 4 (a) shows the change in the threshold of the mCherry laser at pH of 3 - 11. The threshold remained almost unchanged in this pH range. Fig. 4 (b) and (c) show the laser spectra of the mCherry solution at pH 3 and 11. The laser spectra showed slight changes, indicating the good pH stability. In conclusion, the mCherry protein laser showed high stability in a wide pH range, offering considerable potential in the biological detection of liquid environments with different pH levels.

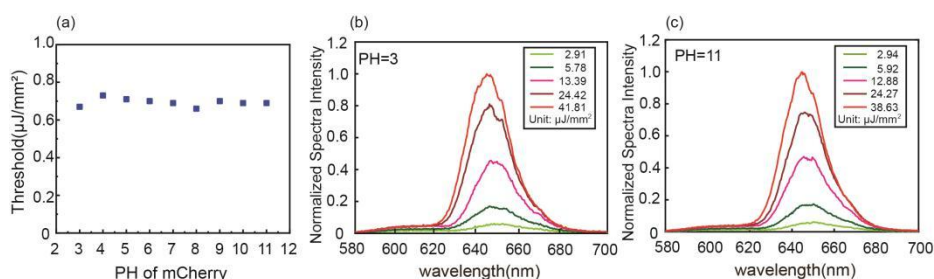


Fig. 4 (a) Threshold of mCherry laser under different pH values; (b) Laser spectra at different pump energy when pH value is 3; (c) Laser spectra at different pump energy when pH value is 10

The laser also showed good photobleaching resistance. The mCherry laser with a threshold of $0.61 \mu\text{J}/\text{mm}^2$ was selected, which was continuously excited using the pump light at $3.54 \mu\text{J}/\text{mm}^2$ for 60 min as shown in Fig. 5 (a). The laser intensity decreased by 54% in the first 10 minutes, and the downward trend gradually decelerate between 10th and 60th minutes. Finally, the intensity decreased by 68% at 60th minute. Fig. 5 (b) shows the green laser generated at the same concentration of the green fluorescent protein (GFP) in the same microcavity. Compared with the mCherry FP laser, the photobleaching effect of the GFP laser is severe and its laser intensity decreased by more than 90% within 10 min of excitation. In contrast, mCherry protein laser has strong optical stability after long-time irradiation of pump light. The good anti-photobleaching effect makes mCherry laser have great practical application prospects.

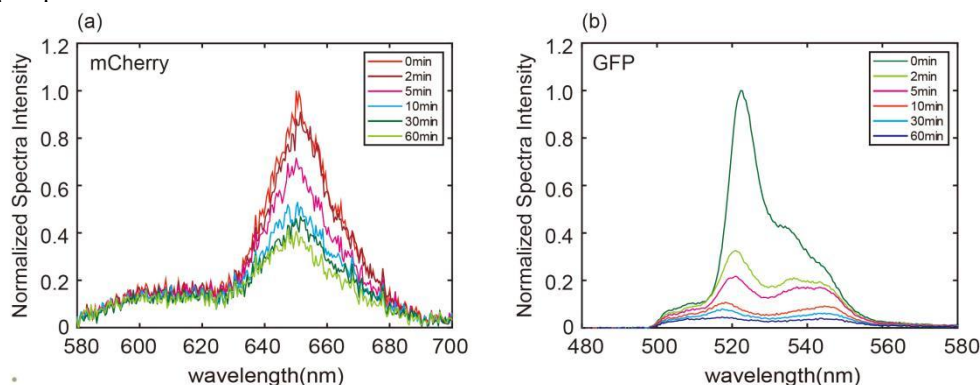


Fig. 5 (a) Laser spectrum change of mCherry laser within 60 minutes under continuous excitation of pump light; (b) At the same concentration, the laser spectrum of GFP laser changes within 60 minutes under the continuous excitation of pump light

Finally, we realized the high-sensitivity detection of the concentration of the mCherry protein solution based on the laser threshold characteristics. Based on the high Q advantage of microcavity, low concentration fluorescent protein gain medium can produce laser, and its detection limit can reach as low as $1.13 \mu\text{M}$ which is the lowest concentration of the gain medium among all currently available FP lasers. Fig. 6 (a), (b) and (c) show the spectrum of mCherry laser with the concentration of $3.31 \mu\text{M}$, $2.65 \mu\text{M}$, and $1.13 \mu\text{M}$ respectively. Figure 6 (d) shows the threshold measurement results of the mCherry lasers at the corresponding gain medium concentrations, reaching thresholds of 9.32 , 11.77 , and $45.44 \mu\text{J}/\text{mm}^2$, respectively. Fig. 6 (e) represents the lasing threshold variation with different concentration of mCherry, which is $1.13 \mu\text{M}$, $1.99 \mu\text{M}$, $2.65 \mu\text{M}$, $3.31 \mu\text{M}$, $4.96 \mu\text{M}$, $6.62 \mu\text{M}$, $9.93 \mu\text{M}$, $19.85 \mu\text{M}$, $39.7 \mu\text{M}$. The corresponding thresholds are $45.44 \mu\text{J}/\text{mm}^2$, $16.72 \mu\text{J}/\text{mm}^2$, $11.77 \mu\text{J}/\text{mm}^2$, $9.32 \mu\text{J}/\text{mm}^2$, $5.34 \mu\text{J}/\text{mm}^2$, $4.08 \mu\text{J}/\text{mm}^2$, $2.26 \mu\text{J}/\text{mm}^2$, $0.97 \mu\text{J}/\text{mm}^2$, $0.59 \mu\text{J}/\text{mm}^2$, respectively. The laser threshold decreased with an increase in the protein concentration.

Therefore, the laser threshold can be used to identify the mCherry protein concentration. The prepared laser can be employed as a high-sensitivity FP concentration detector.

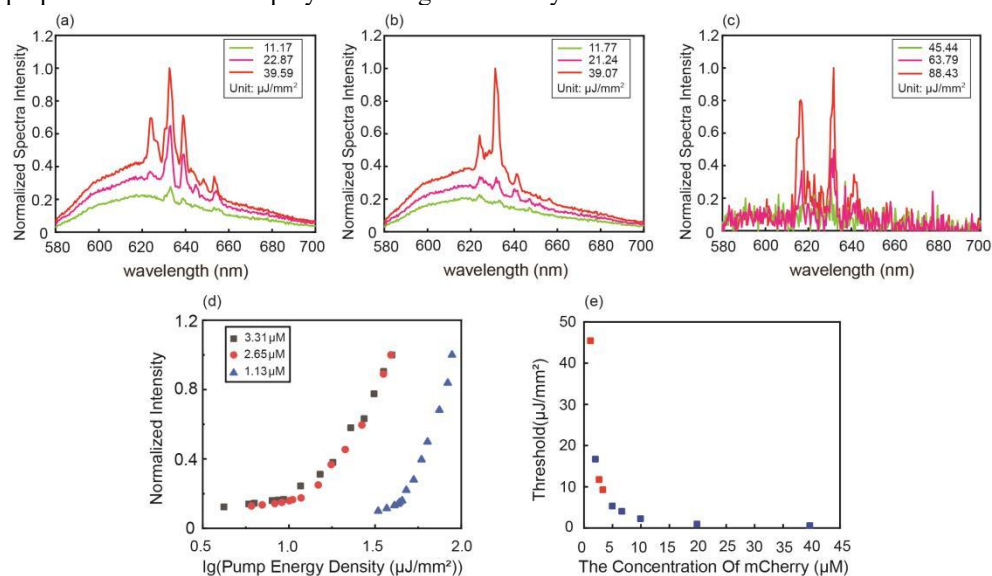


Figure 6 (a) Laser spectra at different pump energy near the threshold when the concentration of mCherry is 3.31 μM ; (b) Laser spectra at different pump energy near the threshold when the concentration of mCherry is 2.65 μM ; (c) Laser spectra at different pump energy near the threshold when the concentration of mCherry is 1.13 μM ; (d) Laser threshold measurement with the concentration of mCherry at 3.31 μM , 2.65 μM , 1.13 μM , respectively; (e) Schematic diagram of laser threshold changing with mCherry concentration, the red dots correspond to concentrations in Fig. 6 (d)

4. Conclusion

A mCherry FP laser was fabricated using mCherry along with a silicon oxide microbubble resonator. The Q factor of the prepared laser reached 10^8 , which is the highest among the currently available FP lasers; furthermore, the corresponding laser threshold is as low as 169 fJ. Owing to the excellent characteristics of mCherry, the laser has good stability. It can be stored at 3 °C for more than one month, and has excellent pH stability from 3 to 11. Furthermore, due to the strong photobleaching resistance of mCherry, the laser can work for a long time under the action of pump light. Red fluorescence could be easily observed in human tissues compared with green fluorescence because of the low absorption rate of red light in human tissues. Therefore, the laser can be used for the biological perception and observation of relevant life activities in deep tissue. Based on its low threshold characteristics, the laser can be used as a mCherry concentration detector whose detection limit can reach as low as 1.13 μM . In future, we plan to use the laser for the detection of trace biomolecules and to study the fluorescence resonance energy transfer.

Funding. China National Postdoctoral Program for Innovative Talents (BX20200057);

Acknowledgement. J. Ma acknowledges financial support from China National Postdoctoral Program for Innovative Talents.

Disclosures. The authors declare no conflicts of interest.

Data availability. Data underlying the results presented in this paper are not publicly available at this time but may be obtained from the authors upon reasonable request.

†These authors contributed equally to this work.

References

1. A. J. C. Kuehne and M. C. Gather, "Organic Lasers: Recent Developments on Materials, Device Geometries, and Fabrication Techniques", *Chem. Rev.* **116**, 12823-12864 (2016).
2. G.-Q. Wei, X.-D. Wang, and L.-S. Liao, "Recent Advances in Organic Whispering-Gallery Mode Lasers", *Laser Photonics Rev.* 2000257 (2020).
3. J. Mysliwiec, K. Cyprych, L. Sznitko and A. Miniewicz, "Biomaterials in light amplification", *J. Opt.* **19**, 033003 (2017).
4. Y.-C. Chen and X. Fan, "Biological Lasers for Biomedical Applications", *Adv. Opt. Mater.* 1900377 (2019).
5. N. Toropov, G. Cabello, M. P. Serrano, R. R. Gutha, M. Rafti and F. Vollmer, "Review of biosensing with whispering-gallery mode lasers", *Light Sci. Appl.* **10**, 42 (2021).
6. G.-Q. Wei, X.-D. Wang, and L.-S. Liao, "Recent Advances in Organic Whispering-Gallery Mode Lasers", *Laser Photonics Rev.* 2000257 (2020).
7. M. Humar and S. H. Yun, "Intracellular microlasers", *Nat. Photon.* **9**, 572-576 (2015).
8. N. Martino, S. J. J. Kwok, A. C. Liapis, S. Forward, H. Jang, H.-M. Kim, S. J. Wu, J. Wu, P. H. Dannenberg, S.-J. Jang, Y.-H. Lee and S.-H. Yun, "Wavelength-encoded laser particles for massively multiplexed cell tagging", *Nat. Photon.* **13**, 720-727 (2019).
9. S. J. J. Kwok, N. Martino, P. H. Dannenberg and S.-H. Yun, "Multiplexed laser particles for spatially resolved single-cell analysis", *Light Sci. Appl.* **8**, 74 (2019).
10. Y.-C. Chen, Q. Chen and X. Fan, "Lasing in blood", *Optica*, **3**, 809-815 (2016).
11. Y. Sun, S. I. Shopova, C.-S. Wu, S. Arnold, and X. Fan, "Bioinspired optofluidic FRET lasers via DNA scaffolds", **107**, 16039-16042 (2010).
12. Z. Yuan, Z. Wang, P. Guan, X. Wu, and Y.-C. Chen, "Lasing-Encoded Microsensor Driven by Interfacial Cavity Resonance Energy Transfer", *Adv. Opt. Mater.* 1901596 (2020).
13. W. Lee, Q. Chen, X. Fan and D. K. Yoon, "Digital DNA detection based on a compact optofluidic laser with ultra-low sample consumption", *Lab Chip*, **16**, 4770-4476 (2016).
14. U. Bog, T. Laue, T. Grossmann, T. Beck, T. Wienhold, B. Richter, M. Hirtz, H. Fuchs, H. Kaltc and T. Mappes, "On-chip microlasers for biomolecular detection via highly localized deposition of a multifunctional phospholipid ink", *Lab Chip*, **13**, 2701-2707 (2013).
15. R. Duan, X. Hao, Y. Li and H. Li, "Detection of acetylcholinesterase and its inhibitors by liquid crystal biosensor based on whispering gallery mode", *Sens. Actuators B Chem.* **308**, 127672 (2020).
16. X. Ouyang, T. Liu, Y. Zhang, J. He, Z. He, A. P. Zhang and H.-Y. Tam, "Ultrasensitive optofluidic enzyme-linked immunosorbent assay by on-chip integrated polymer whispering-gallery-mode microlaser sensors", *Lab Chip*, **20**, 2438-2446 (2020).
17. L. He, S. K. Ozdemir, J. Zhu, W. Kim and L. Yang, "Detecting single viruses and nanoparticles using whispering gallery microlasers", *Nat. Nanotechnol.* **6**, 428 - 432 (2011).
18. S. Vincent, S. Subramanian and F. Vollmer, "Optoplasmonic characterisation of reversible disulfide interactions at single thiol sites in the attomolar regime", *Nat. Commun.* **11**, 2043 (2020).
19. Z. Guo, Y. Qin, P. Chen, J. Hu, Y. Zhou, X. Zhao, Z. Liu, Y. Fei, X. Jiang, and X. Wu, "Hyperboloid-Drum Microdisk Laser Biosensor for Ultrasensitive Detection of Human IgG", *Small* 2000239 (2020).
20. L. Shao, X.-F. Jiang, X.-C. Yu, B.-B. Li, W. R. Clements, F. Vollmer, W. Wang, Y.-F. Xiao, and Q. Gong, "Detection of Single Nanoparticles and Lentiviruses Using Microcavity Resonance Broadening", *Adv. Mater.* **25**, 5616-5620, (2013).

21. Y.-C. Chen, X. Tan, Q. Sun, Q. Chen, W. wang and X. Fan, "Laser-emission imaging of nuclear biomarkers for high-contrast cancer screening and immunodiagnosis", *Nat. Bio. Engineering*, **1**, 724-735 (2017).
22. G. Patterson, R. N. Day, D. Piston, "Fluorescent protein spectra", *J. Cell Sci* **114**, 837-838 (2001).
23. M. C. Gather, S. H. Yun, "Single-cell biological lasers", *Nat. Photon.* **5**, 406-410 (2011).
24. C. P. Dietrich, S. Hofling, and M. C. Gather, "Multi-state lasing in self-assembled ring-shaped green fluorescent protein microcavities", *Appl. Phys. Lett.* **105**, 233702 (2014).
25. C. P. Dietrich, A. Steude, L. Tropsch, M. Schubert, N. M. Kronenberg, K. Ostermann, S. Hofling, C. M. Gather, "An exciton-polariton laser based on biologically produced fluorescent protein", *Sci. Adv.* **2**, e1600666 (2016).
26. I. B. Dogru, K. Min, M. Umar, H. B. Jalali, E. Begar, D. Conkar, E. N. F. Karalar, S. Kim, and S. Nizamoglu, "Single transverse mode protein laser", *Appl. Phys. Lett.* **111**, 231103 (2017).
27. M. Karl, A. Meek, C. Murawski, L. Tropsch, C. Keum, M. Schubert, I. D. W. Samuel, G. A. Turnbull, and M. C. Gather, "Distributed Feedback Lasers Based on Green Fluorescent Protein and Conformal High Refractive Index Oxide Layers", *Laser Photonics Rev.* **14**, 2000101 (2020).
28. M. Gather, S. Yun, "Bio-optimized energy transfer in densely packed fluorescent protein enables near-maximal luminescence and solid-state lasers". *Nat Commun* **5**, 5722 (2014).
29. Q. Chen, M. Ritt, S. Sivaramakrishnan, Y. Sun and X. Fan, "Optofluidic lasers with a single molecular layer of gain", *Lab Chip*, **14**, 4590-4595 (2014).
30. A. Jonáš, M. Aas, Y. Karadag, S. Manioğlu, S. Anand, D. McGloin, H. Bayraktarc and A. Kiraz, "In vitro and in vivo biolasing of fluorescent proteins suspended in liquid microdroplet cavities", *Lab Chip*, **14**, 3093-3100 (2014).
31. Q. Chen, X. Zhang, Y. Sun, M. Ritt, S. Sivaramakrishnan, X. Fan, "Highly sensitive fluorescent protein FRET detection using optofluidic lasers", *Lab Chip* **13**, 2679-2681 (2013).
32. N. C. Shaner, R. E. Campbell, P. A. Steinbach, B. N. G. Giepmans, A. E. Palmer and R. Y. Tsien, "Improved monomeric red, orange and yellow fluorescent proteins derived from *Discosoma* sp. red fluorescent protein", *Nat. Biotechnol.* **22**, 1567 - 1572 (2004).
33. M. Sumetsky, Y. Dulashko, and R. S. Windeler, "Optical microbubble resonator", *Opt. Lett.* **35**, 898-900 (2010).
34. F. V. Subach, G. H. Patterson, S. Manley, J. M. Gillette, J. Lippincott-Schwartz and V. V. Verkhusha, "Photoactivatable mCherry for high-resolution two-color fluorescence microscopy", *Nat. Methods*, **6**, 153 - 159 (2009)..
35. B. Wu, Y. Chen and J. D. Müller, "Fluorescence Fluctuation Spectroscopy of mCherry in Living Cells", *Biophys. J.* **96**, 2391-2404 (2009).
36. J.-Y. Fan, Z.-Q. Cui, H.-P. Wei, Z.-P. Zhang, Y.-F. Zhou, Y.-P. Wang, X.-E. Zhang, "Split mCherry as a new red bimolecular fluorescence complementation system for visualizing protein - protein interactions in living cells", *Biochem. Biophys. Res. Commun.* **367**, 47-53 (2008).
37. X. Shu, N. C. Shaner, C. A. Yarbrough, R. Y. Tsien and S. J. Remington, "Novel chromophores and buried charges control color in mFruits", *Biochemistry*, **45**, 9639-9647 (2006).
38. F. Yang, L. G. Moss, G. N. Philips Jr., "The molecular structure of green fluorescent protein", *Nat. Biotechnol.* **14** 1246-1251 (1996).
39. F. Neese, F. Wennmohs, U. Becker, C. Riplinger, "The ORCA quantum chemistry program package", *J. Chem. Phys.* **152** 224108 (2020).
40. Shaner Nc, Campbell Re, Steinbach Pa, Giepmans Bng, Palmer Ae, Tsien Ry, "Improved monomeric red, orange and yellow fluorescent proteins derived from *Discosoma* sp. red fluorescent protein", *Nature Biotechnology*, **22** , 1567-1572.(2004).